THE ASTROPHYSICAL JOURNAL, 420:341–347, 1994 January 1

THEORETICAL LIGHT CURVES OF TYPE IIb SUPERNOVA 1993J

TOSHIKAZU SHIGEYAMA, TOMOHARU SUZUKI, SHIOMI KUMAGAI, AND KEN'ICHI NOMOTO
Department of Astronomy, School of Science, University of Tokyo, Tokyo 113, Japan

HIDEYUKI SAIO
Department of Astronomy, Faculty of Science, Tohoku University, Sendai 980, Japan

AND

HITOSHI YAMAOKA
Department of Physics, College of General Education, Kyushu University, Fukuoka 810, Japan
Received 1993 May 24; accepted 1993 June 30

ABSTRACT

The observed feature of the light curve of SN 1993J, which has two maxima, are shown to be well reproduced by the explosion of red supergiant if its H/He envelope mass has been decreased below $\sim 0.9\ M_\odot$. The first maximum of the light curve is due to shock heating of the thin envelope, while the second maximum is due to the radioactive decay of ^{56}Co. From the date of the second maximum, the progenitor's main-sequence mass is estimated to be ~ 12–$15\ M_\odot$. The thin envelope is likely to be the result of a close binary evolution. The mass of ^{56}Ni synthesized in SN 1993J is $\sim 0.08\ M_\odot$. The light curve properties, in particular, the date of the minimum, and the decline rate of the tail suggest that substantial ^{56}Ni was mixed into helium layers as has been predicted for Type Ib/Ic supernovae. We also calculate the light curves of line γ-rays as well as the spectral evolution of hard X-rays resulting from the ^{56}Ni–^{56}Co decays and discuss the possibility of observing hard radiation with the *Compton Gamma-Ray Observatory*. We show that hard X-rays from the pulsar can be observed with *ASCA* in ~ 3 years if the pulsar luminosity is as high as the Crab Nebula.

Subject headings: binaries: general — nuclear reactions, nucleosynthesis, abundances — stars: evolution — stars: interiors — supernovae: general — supernovae: individual (SN 1993J)

1. INTRODUCTION

SN 1993J in M81 (NGC 3031) was discovered in the very early rising phase (Garcia 1993) and its detailed light curve has been constructed from extensive photometric observations (e.g., van Driel et al. 1993; Schmidt et al. 1993). SN 1993J was identified as a Type II supernova (SN II) (Filippenko 1993a; Garnavich & Ann 1993; Taniguchi et al. 1993). Previously SNe II have been subclassified into a plateau type (SN II-P) and a linear decline type (SN II-L) according to the light curve shape (e.g., Dogget & Brnach 1985). The light curve of SN 1993J shows a distinct difference from those of previously known SNe II, as it shows neither a clear plateau nor a monotonic decline. In fact, SN 1993J quickly reached the first maximum, declined in ~ 5 days, rose to a second maximum in ~ 10–15 days depending on the wavelength, and then declined again.

To identify the energy source of such an unusual light curve, the best way is to compare the observed and theoretical *bolometric* light curves. The bolometric light curve of SN 1993J has been constructed by Schmidt et al. (1993) using *BVI* photometry and bolometric corrections derived from models and SN 1987A; the distance to SN 1993J and the extinction are assumed to be 3.3 Mpc and $A_v = 0.4$ mag, respectively.

Nomoto et al. (1993) have pointed out that the bolometric light curve of SN 1993J around the second maximum is in striking agreement with that of the Type Ib supernova (SN Ib) 1983N as well as its helium star models (Shigeyama et al. 1990). This implies that the light curve of SN 1993J has been powered by the decay of ^{56}Co after the first minimum. From the width of the second peak which is approximately given as $\Delta t_{\rm peak} \propto \bar{\kappa}^{1/2} M_{\rm ej}^{3/4} E^{-1/4}$ by equating the diffusion timescale to the dynamical timescale of the ejecta (Arnett 1982), the total ejecta mass of SN 1993J is estimated to be as small as $M_{\rm ej} \sim 4\ M_\odot$ (here $\bar{\kappa}$ and E denote the mean opacity and kinetic energy of explosion, respectively). The observed spectral features have changed from SN II to SN Ib (Filippenko & Matheson 1993), so that SN 1993J can be classfied as a Type II-b supernova (SN II-b) (Woosley, Pinto, & Ensman 1988; Filippenko 1988; Woosley 1991). From the date of the second maximum Nomoto et al. (1993) have also suggested that the progenitor lost most of its envelope by a binary interaction. Podsiadlowski et al. (1993) and Woosley (1993) have reached similar conclusions.

Here we present detailed hydrodynamical models of SNe II-b, i.e., explosions of stars that have low-mass H/He envelopes. Hydrodynamics of explosion is discussed in § 2 and the theoretical optical light curves are presented in § 3. We demonstrate that mixing of ^{56}Ni within the helium core has an important effect on the light curve, and suggest that SN 1993J has actually undergone such mixing. We then calculate the light curves of line γ-rays and hard X-rays from SN 1993J and discuss the possibility of those lines being observed (§ 4). We also calculate the emergent X-ray spectra from the pulsar and discuss the observability with ASCA (§ 5).

2. HYDRODYNAMICAL MODELS

To set up the initial model of explosion, we use a presupernova model of the 4 $M_\odot$ helium star that has formed from the main-sequence star of $M_{\rm ms} = 15\ M_\odot$ (with the solar metallicity) and evolved from helium burning through collapse (Nomoto & Hashimoto 1988). The adopted main-sequence mass is consistent with the inferred progenitor's luminosity

TABLE 1

MODELS FOR SN 1993J

Name	$M_{env}/M_{\odot}$	$R/R_{\odot}$	$L/L_{\odot}$	T_{eff} (K)	Y	E (ergs)
4H89.........	0.89	300	6.8×10^4	5400	0.80	1.2×10^{51}
4H47.........	0.47	350	6.8×10^4	5000	0.79	1.0×10^{51}
4H39.........	0.39	250	6.8×10^4	5900	0.80	1.2×10^{51}

(Hashimoto, Iwamoto, & Nomoto 1993). A hydrostatic and thermal equilibrium H/He envelope is constructed to fit to the helium star smoothly in the middle of the helium layer. The envelope models with various masses M_{env} and radii R are constructed by varying the mass fraction of helium Y in the envelope of a uniform composition (see, e.g., Saio, Kato, & Nomoto 1988a). The parameters of three particular models 4H89, 4H47, and 4H39 used here are summarized in Table 1 and the density distributions are shown in Figure 1.

These models have large helium abundances. Such an enhancement of helium is expected from the gradient of helium abundance in the deepest layers of the envelope (see, e.g., Saio, Nomoto, & Kato 1988b); if most of the outer part of the envelope is removed, the helium-rich layer is exposed. Though these models are a little bluer than a K0 supergiant suggested for the most likely progenitor, it may be consistent in view of large uncertainties in the identification of the progenitor including the possibility that it is not the K0 supergiant (Perelmuter 1993; Filippenko 1993b; Humphreys et al. 1993).

The hydrodynamics of explosion is simulated by depositing energy to generate a strong shock wave around the outer edge of the 1.3 $M_{\odot}$ Fe core as in Shigeyama & Nomoto (1990) except for replacing the hydrodynamical code with the PPM scheme (Colella & Woodward 1984). Nucleosynthesis results are nearly the same as described in Shigeyama et al. (1990) and Thielemann, Nomoto, & Hashimoto (1993). The model parameters such as the deposited energy and the mass cut are set to produce the kinetic energy of explosion given in Table 1 and 0.075 $M_{\odot}$ ^{56}Ni. Other heavy elements synthesized in the helium core include: 0.0033 $M_{\odot}$ Ca, 0.0040 $M_{\odot}$ Ar, 0.023 $M_{\odot}$ S, 0.071 $M_{\odot}$ Si, 0.046 $M_{\odot}$ Mg, 0.039 $M_{\odot}$ Ne, 0.433 $M_{\odot}$ O, and 0.063 $M_{\odot}$ C. The determination of oxygen mass from the late-time spectra would be particularly important to identify the progenitor's mass, since the produced oxygen masses are 0.218 and 1.48 $M_{\odot}$ for the helium cores of 3.3 and 6 $M_{\odot}$, respectively, and thus sensitive to the core mass (Thielemann et al. 1993).

When the shock wave hits the He/C+O interface, the expansion of the Si/O/C core is decelerated to generate a reverse shock (Shigeyama et al. 1990). This should induce a certain degree of mixing due to the Rayleigh-Taylor instability (Hachisu et al. 1991). How much ^{56}Ni is mixed into the helium layer depends on the pre-mixing of ^{56}Ni due to neutrino-induced Rayleigh-Taylor instabilities (Hachisu et al. 1993). In view of such uncertainties, we explore two extreme cases of mixing, i.e., with complete mixing interior to the H/He interface and without mixing.

The Rayleigh-Taylor instability at the H/He interface is weak because the deceleration of the core expansion is smaller due to the low envelope mass (Hachisu et al. 1991, 1994). For simplicity, therefore, we assume that there is no mixing between the H-rich envelope and the core. However, a certain degree of mixing between the H-rich envelope and the helium layer would be inevitable because of the large density jump across the low-density envelope and the core (Hachisu et al. 1994; Hashimoto et al. 1993), which may affect the light curve shape around the second maximum (Shigeyama & Nomoto 1990, 1991).

The shock wave propagates rather fast through the low-density envelope and arrives at the stellar surface in 0.16 days after the core collapse for model 4H89, 0.21 days for 4H47, and 0.11 days for 4H39. Differing from the model for SN 1987A, the expansion of the helium core does not become homologous even at day ~40. The density distributions as a function of the expansion velocity at a homologously expanding stage (day 80) are shown in Figure 2 for 4H89 (*solid line*) and 4H47 (*dashed line*) where the density scales as t^{-3} with t being the time after

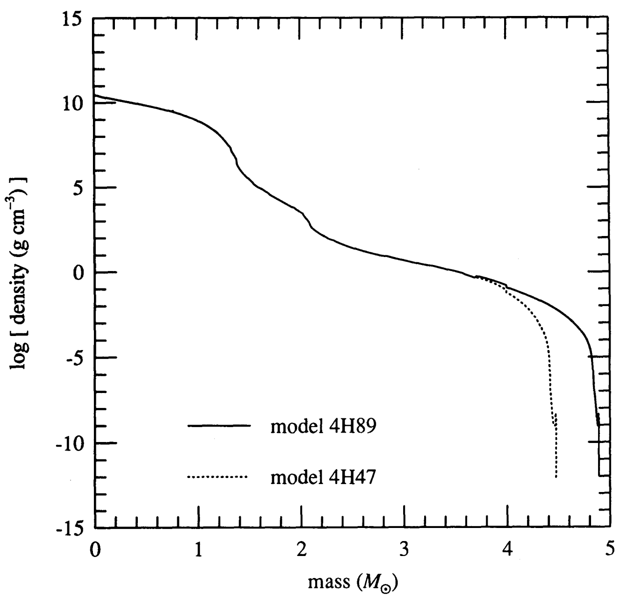

FIG. 1.—Presupernova density distributions of models 4H89 (*solid curve*) and 4H47 (*dashed curve*) against the enclosed mass.

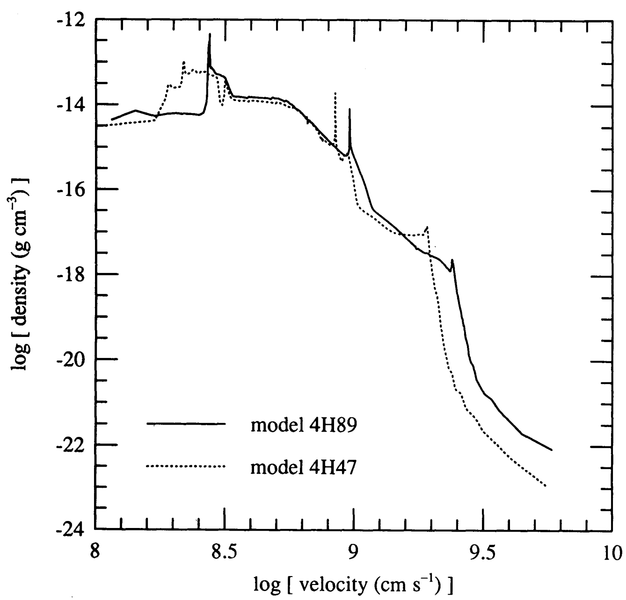

FIG. 2.—Density distributions against the expansion velocity at day 80 since explosion for 4H89 (*solid lines*) and 4H47 (*dashed lines*).

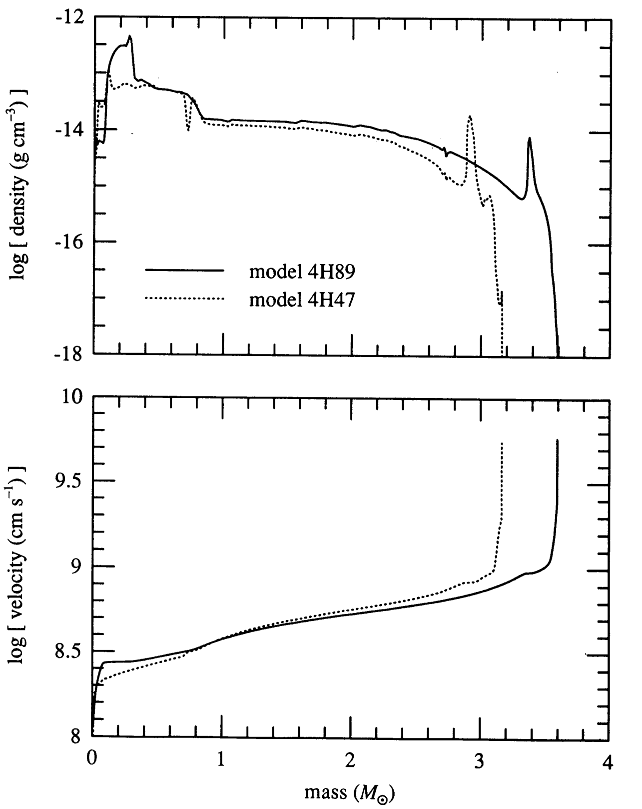

FIG. 3.—Density (*upper*) and velocity (*lower*) distributions against the enclosed mass at day 80 for 4H89 (*solid lines*) and 4H47 (*dashed lines*).

the explosion. In the outer layers, the density gradient $n = -d \ln \rho / d \ln v$ is as steep as $n \sim 20$ (4H89) and 25 (4H47). The density and velocity distributions against the enclosed mass are shown in Figure 3. The velocity at the bottom of the H-rich envelope $v_{\mathrm{H,min}}$ is 6500 km s^{-1} (4H89) and 7500 km s^{-1} (4H47).

Comparison with the SN Ib model light curves of bare helium stars with $E = 1 \times 10^{51}$ ergs (Shigeyama et al. 1990; Nomoto et al. 1993) is useful to understand the effect of the hydrogen-rich envelope on the hydrodynamics and the light curve. The kinetic energies of the helium core (and the ratio to the total energies) in the models 4H89 and 4H47 are 5.6×10^{50} ergs (0.47) and 5.8×10^{50} ergs (0.58), respectively. They are significantly smaller than those in the bare helium star models due to the deceleration of the core expansion by the envelope.

3. OPTICAL LIGHT CURVE

Theoretical light curves after the shock breakout including radioactive decays of 0.075 $M_\odot$ ^{56}Ni and ^{56}Co are calculated as in Shigeyama & Nomoto (1990). For radiative transfer, we apply the flux limited diffusion approximation. For Thomson scattering opacity, the electron mole number is obtained by solving Saha equations for hydrogen, helium, and oxygen with their appropriate mixture. For the absorptive opacities we set the Rosseland mean opacities $0.009Y + 0.01Z$ cm^2 g^{-1}, where Z denotes the mass fraction of heavy elements.

The early light curve through the first minimum at $t \sim 7$ days can be accounted for by the diffusive release of the internal energy of the radiation field established by the shock wave. The bolometric luminosity reaches the first maximum of $L = 4.6 \times 10^{45}$ ergs s^{-1} at $t = 0.16$ days in model 4H89 and $L = 3.7 \times 10^{45}$ ergs s^{-1} at $t = 0.2$ days in model 4H47. Figures 4*a* and 5*a* show that the calculated light curves through the minimum for models 4H89 and 4H47 are in reasonably good agreement with SN 1993J. Because of the small envelope mass and the enhanced helium abundance in the envelope, the photospheric temperature decreases to $\sim 10^4$ K in a week after the explosion (see Figs. 4*b* and 5*b*). At the light curve minimum, hydrogen ions already started to recombine. For model 4H39 (long dashed line in Fig. 5*a*), the light curve declines too fast. For such a small mass envelope, the radius should be larger to be consistent with SN 1993J (Podsiadlowski et al. 1993; Woosley 1993).

At the light curve minimum, heating due to radioactive decays begins to brighten the supernova. The date when this heating effect appears in the light curve depends on the extent of ^{56}Ni mixing as shown for the cases with mixing (*solid lines*) and without mixing (*dashed lines*) in Figures 4*a* and 5*a*. With mixing of ^{56}Ni, heating effect starts earlier, so that the minimum of the light curve is reached at $t = 6$ days (with mixing) and $t = 10$ days (no mixing) in Figure 4*a*. It is clear that the light curve with mixing is in much better agreement with SN 1993J than without mixing for both 4H89 and 4H87. Even with mixing, the diffusion time for photons in the hydrogen-rich envelope of 4H89 is too long to brighten the supernova at the observed minimum luminosity (Fig. 4*a*), while model 4H47 with a smaller mass hydrogen-rich envelope can reproduce the observed minimum luminosity (Fig. 5*a*). A similar effect of heating was seen in the light curve of SN 1987A around day 25 (Shigeyama & Nomoto 1990). In SN 1993J, the envelope is so thin in mass that the effect appears much earlier.

As the heating wave due to the ^{56}Ni–^{56}Co decays propagates outward, the hydrogen recombination front moves outward in radius (see Shigeyama & Nomoto 1990, 1991). The associated expansion of the photosphere leads to the increase in the luminosity. The light curve reaches the second maximum when all the hydrogen ions have recombined. The photosphere enters the helium layer at this moment. With mixing of ^{56}Ni, the luminosity increases more slowly, reaches the second maximum earlier, and forms a broader peak, which is in much better agreement with SN 1993J than the case with no mixing. Similar dependence of the light curve shape on the mixing was found for SN 1987A (e.g., Shigeyama & Nomoto 1990).

The bolometric luminosity at the second maximum depends on the minimum expansion velocity of hydrogen $v_{\mathrm{H,min}}$ as (Shigeyama & Nomoto 1990, 1991)

$$L_{\mathrm{bol}} = 4\pi\sigma v_{\mathrm{H,min}}^2 t_{\mathrm{max}}^2 T_{\mathrm{eff}}^4, \sim 2.5 \times 10^{42} \text{ ergs s}^{-1} .$$

Here we apply the effective temperature $T_{\mathrm{eff}} \sim 6500$ K, the date of the second maximum $t_{\mathrm{max}} \sim 22$ days and $v_{\mathrm{H,min}} \sim 7500$ km s^{-1}, which approximately reproduces the calculated maximum luminosity in Figure 5*a*. Figures 4*a* and 5*a* show that both models have too large $v_{\mathrm{H,min}}$ to be consistent with the observed luminosity. It is therefore likely that some mixing has taken place around the H/He interface to lower $v_{\mathrm{H,min}}$ in both models. Alternatively the explosion energy of this supernova was significantly less than 10^{51} ergs. Multidimensional hydrodynamical calculations for explosion of stars like models 4H89 and 4H47 are necessary to find out to what extent hydrogen is mixed into the helium layer. Such an effect of hydrogen mixing on the maximum luminosity has been found for SN 1987A (Shigeyama & Nomoto 1990).

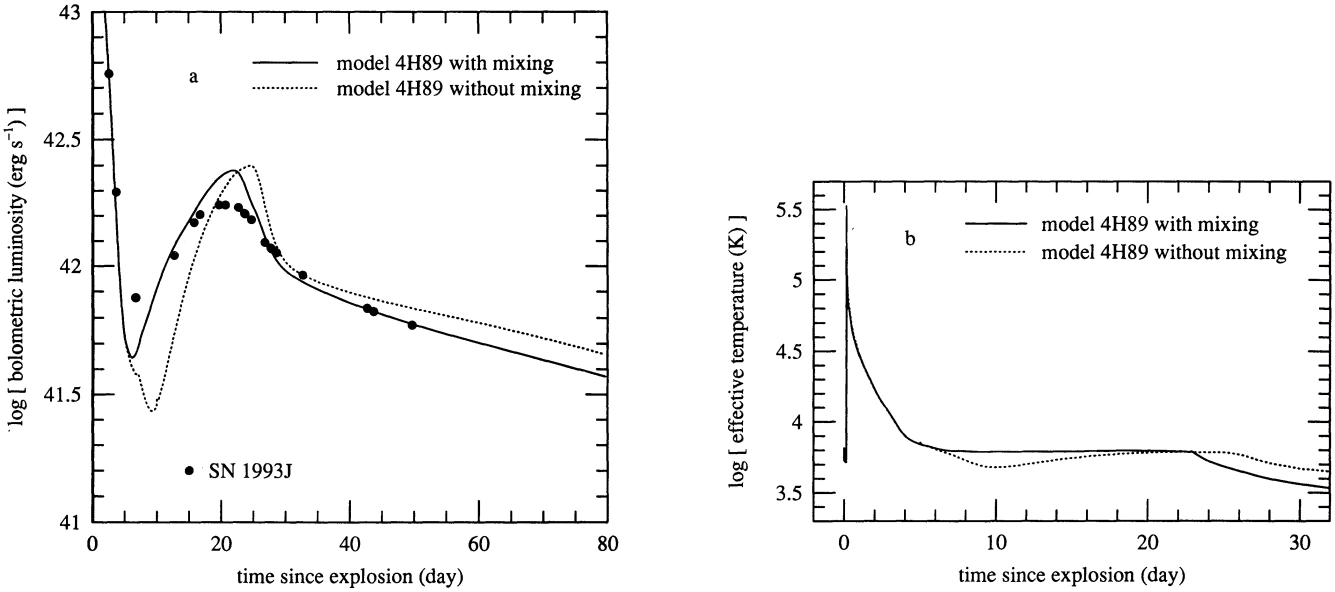

FIG. 4.—Calculated light curves (*a*) and effective temperatures (*b*) for model 4H89 with $M_{env} = 0.89\ M_{\odot}$. The solid and the dashed lines show the cases with mixing inside the He core and without mixing, respectively. The bolometric light curve of SN 1993J is shown by the filled circles.

The calculated light curve enters the tail of the ^{56}Co decay at $t \sim 25$ days for both models. The decline is faster with mixing than without mixing because more γ-rays escape from the star before thermalized. The decline rate with mixing is again in much better agreement with the observation than without mixing. Figure 6 shows the total energy generation rate of the ^{56}Ni and ^{56}Co decays (*thick solid line*), X-ray/γ-ray light curves, and the UVOIR bolometric light curves for 4H47 (with and without ^{56}Ni mixing shown by the solid and dotted lines, respectively) and 4H89 (with and without mixing shown by the dash-dotted and the dashed lines, respectively). The decline rate of the light curve tail is slower in these SNe II-b models than in the SNe Ib models because of slower γ-ray escape from the decelerated helium core (§ 2).

From the date of the second maximum of the light curve ($t \sim 22$ days), the helium core mass of the progenitor of SN 1993J can be estimated as $M_{\alpha} = 3$–$6\ M_{\odot}$ (Nomoto et al. 1993); the light curve of the 6 $M_{\odot}$ helium star reaches the maximum at day 20 and 25 with and without mixing, respectively (Shigeyama et al. 1990), so that more massive star models cannot be consistent with SN 1993J.

4. γ-RAY LIGHT CURVE

SN 1993J provides the *Compton Gamma-Ray Observatory* (*CGRO*) with an interesting possibility of line γ-ray observations. If the lines are detected, it will be another direct confirmation of the synthesis of radioactive ^{56}Ni in SNe II as first made with SN 1987A. Though the distance to SN 1993J is 66 times longer than SN 1987A, the column density of the ejecta of model 4H47 is 70 g cm^{-2} at $t = 80$ days, which is only $\sim\frac{1}{4}$

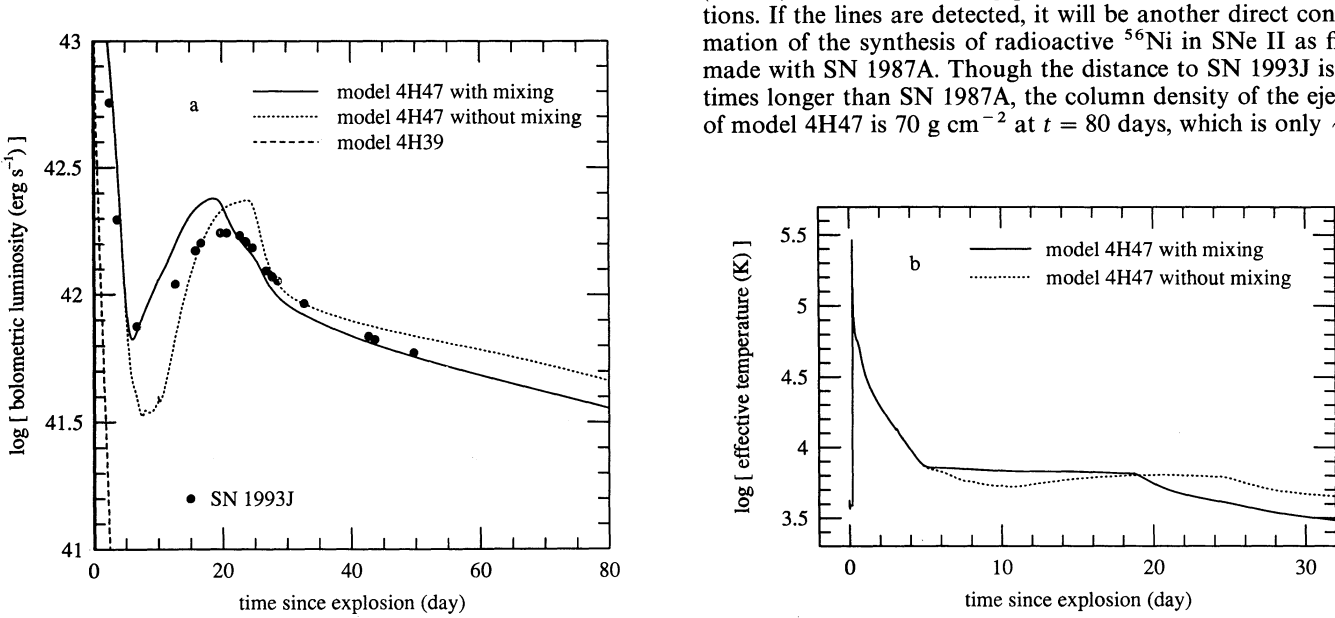

FIG. 5.—Calculated light curves (*a*) and effective temperatures (*b*) for model 4H47 with the envelope mass $M_{env} = 0.47\ M_{\odot}$. The early part of the light curve of model 4H39 with $M_{env} = 0.39\ M_{\odot}$ is shown by the long dashed curve.

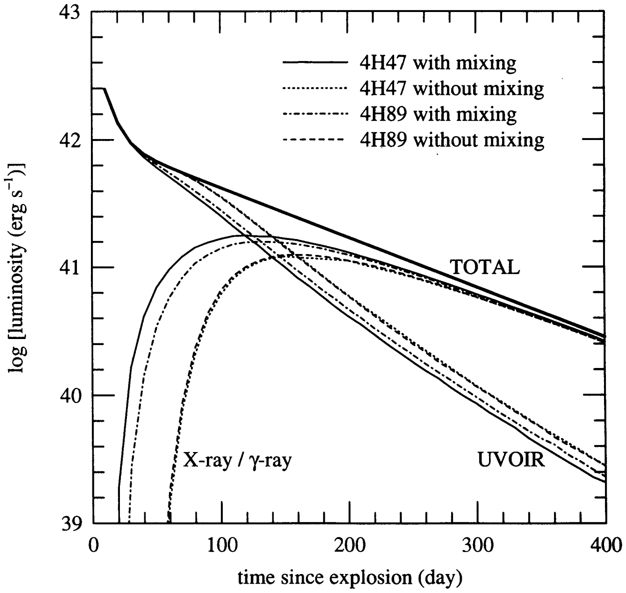

FIG. 6.—Total energy generation rate of the ^{56}Ni and ^{56}Co decays (*thick solid line*), *X*-ray/γ-ray light curves, and UVOIR bolometric light curves for 4H47 (with and without ^{56}Ni mixing shown by the solid and dotted lines, respectively) and 4H89 (with and without mixing shown by the dash-dotted and dashed lines, respectively). The mass of ^{56}Ni is 0.075 $M_\odot$.

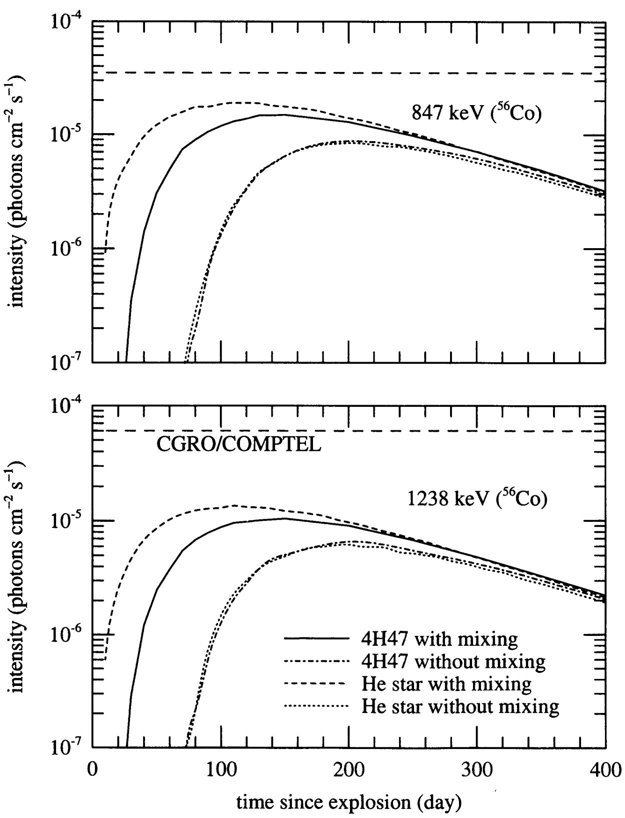

FIG. 7.—Line γ-ray light curves expected from SN 1993J as compared with the detection limit of the *CGRO*/COMPTEL experiment (*long-dashed lines*). Two cases with and without ^{56}Ni mixing are shown. The upper part shows light curves of 847 keV lines from model 4H47 with mixing (*solid curve*) and without mixing (*dash-dotted curve*). Also shown are the 847 keV light curves from the explosion of the 4 $M_\odot$ He star with and without mixing. The lower part is for 1238 keV. The ^{56}Ni mass is 0.075 $M_\odot$. The assumed distance to SN 1993J is 3.3 Mpc.

of the model 14E1 for SN 1987A (Nomoto, Kumagai, & Shigeyama 1991) because of the significantly faster expansion of SN 1993J than SN 1987A due to the smaller mass envelope. Earlier calculations have shown that *CGRO* could detect the line γ-rays from SNe Ia and Ib/Ic but not from ordinary SNe II-P at the distance of 3.3 Mpc (Kumagai, Shigeyama, & Nomoto 1991; Nomoto et al. 1991; The, Clayton, & Burrows 1991).

Figure 7 shows the light curves of γ-ray lines (847 and 1238 keV) calculated with Monte Carlo simulations (Kumagai et al. 1989) for the model 4H47 with and without mixing of ^{56}Ni as well as those for the 4 $M_\odot$ helium star. The helium star model corresponds to the case of extremely small envelope mass. The flux and the date of maximum depend on the mass of ^{56}Ni and mixing. Mixing of ^{56}Ni throughout the helium layer makes the maximum earlier ($\sim$130 days) compared with the unmixed case ($\sim$200 days). The maximum fluxes of these models with 0.075 $M_\odot$ ^{56}Ni are lower than the detection limit of the *CGRO*/COMPTEL experiment (the dashed line in Fig. 7; Schönfelder et al. 1993) by a factor of $\sim$2.

However, the ^{56}Ni mass estimate is subject to uncertainties involved in the extinction and the bolometric correction. If the extinction is as large as $A_v = 1.0$ mag (Humphreys et al. 1993) rather than the adopted value of 0.4 mag, the ^{56}Ni mass is $\sim$0.13 $M_\odot$. The adopted bolometric correction is uncertain because of the small envelope mass and helium enhancement (Schmidt et al. 1993). If ^{56}Ni is mixed as suggested from the present optical light curve models, therefore, the γ-ray lines from SN 1993J could marginally be observed with the *CGRO*/COMPTEL experiment around day 130 days.

CGRO may also be able to observe the Compton-degraded hard X-rays. Figure 8 shows the evolution of the hard X-ray spectrum calculated with Monte Carlo simulations (Kumagai et al. 1989) for 4H47. The X-ray flux reaches maximum around $t \sim 100$ days, which is lower than the detection limit of the OSSE experiment (Johnson et al. 1993) by a factor of 3.

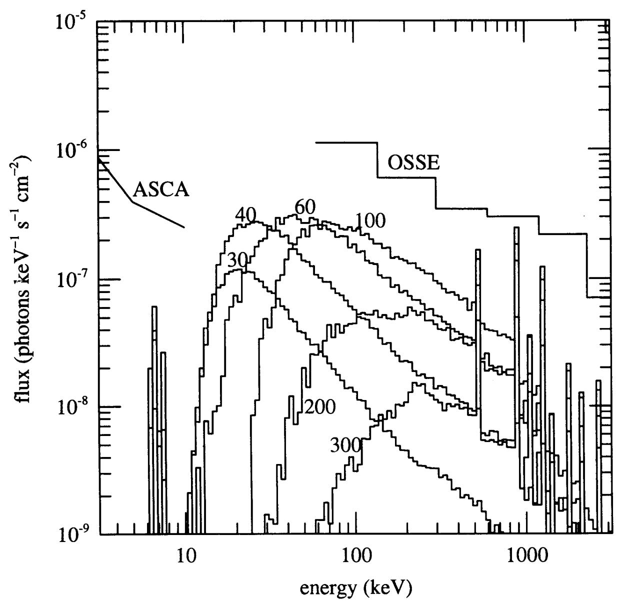

FIG. 8.—Evolution of the hard X-ray spectrum calculated with Monte Carlo simulations for 4H47. The ^{56}Ni mass is 0.075 $M_\odot$. The X-ray flux reaches maximum around $t \sim 100$ days. The dates are indicated by numbers. The detection limits with the ASCA (Inoue et al. 1991) and the OSSE experiment (Schönfelder et al. 1993) are shown.

5. POSSIBLE SIGNALS FROM A PULSAR

The relatively small mass progenitor as inferred in § 3 is likely to form a neutron star rather than a black hole. Since the magnetic field strength and the rotation period of a new-born neutron star are unknown, it is useful to predict the possibilities to observe the pulsar activity in optical and X-ray wavebands.

Figure 9 shows the optical light curve of 4H89 which has an additional energy source of a central pulsar. Three curves are for various values of pulsar luminosity $L_{\rm pul}$ from 2×10^{41} to 3×10^{40} ergs s^{-1}. If $L_{\rm pul} \gtrsim 1 \times 10^{41}$ ergs s^{-1}, its heating effect could have broadened the second maximum; it would also slow down the decline in the tail, though the decline is still faster than the curve for which all γ-rays from the decay of 0.075 $M_\odot$ ^{56}Co are assumed to be thermalized (*thick solid line*). Therefore, the pulsar contribution to the bolometric light curve may not be easily distinguished from the ^{56}Co decay tail until $t \sim 80$ days. However, it is interesting that SN 1993J has brightened in U band, which might be a signal from the pulsar, although the luminosites in other bands are still falling (Tweedy et al. 1993; Wheeler et al. 1993). For a longer term, the decline rate of the light curve would be significantly slowed down as compared with the curves in Figure 6 and the effect of pulsar could be observable. The slow down of the light curve decline is also expected to occur due to the delayed recombination (Fransson & Kozma 1993) which would be more significant in SN 1993J than SN 1987A because of the faster expansion.

In X-ray bands, the observation of a pulsar with ASCA (Tanaka 1993) would be possible. For SN 1987A Kumagai et al. (1993) have shown that, if the pulsar luminosity in the 1 keV to 10 MeV range exceeds $\sim 5 \times 10^{35}$ ergs s^{-1}, the X-rays from the pulsar could be detected with ASCA in the 5–10 keV band $\gtrsim 8$ years after the explosion. For SN 1993J the photoelectric absorption at 5–10 keV can become small enough for the pulsar observations at $t \gtrsim 3$ years, within the ASCA life time. Figure 10 shows the evolution of the emergent hard X-ray spectrum of the radiation from a pulsar. Here the spectrum of the pulsar radiation is assumed to be power law with photon index 2.2 and the luminosity in the 1 keV to 10 MeV range is 5×10^{38} ergs s^{-1}. If the hard X-ray luminosity of the SN 1993J pulsar is similar to the Crab Nebula, therefore, the hard X-rays can be observed at $t \gtrsim 3$ years. Since most of photons are unscattered, the determination of the pulsar periodicity is possible (Kumagai et al. 1993). Even the lower luminosity pulsar could be observed with future missions such as ASTRO-E.

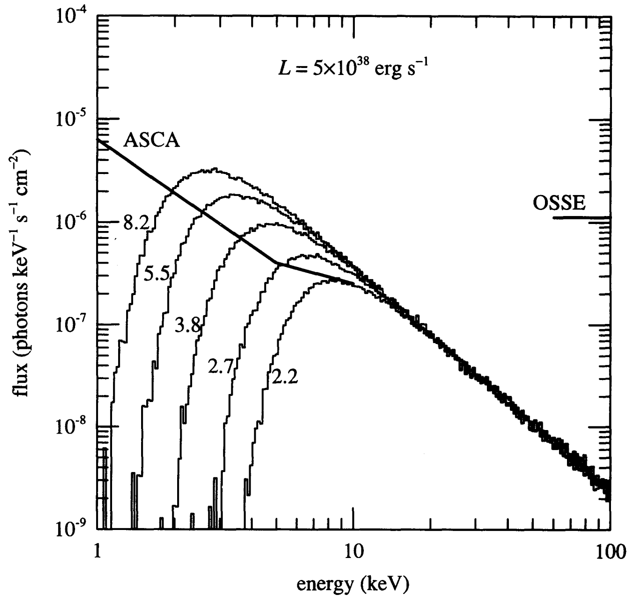

FIG. 10.—Evolution of emergent spectra from a radiation source embedded in the ejecta model 4H47. The age after core collapse is indicated by numbers (in years). The radiation source has a power-law spectrum with a photon index 2.2 in the 1 keV to 10 MeV range. The luminosity from this source in this energy range is assumed to be 5×10^{38} ergs s^{-1}.

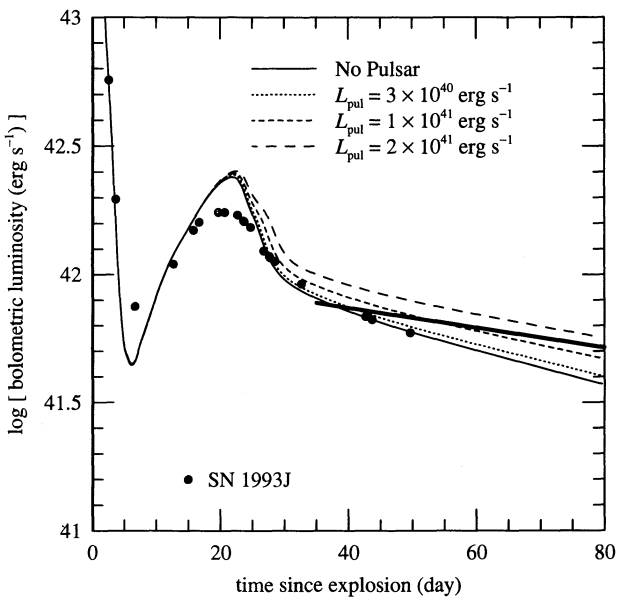

FIG. 9.—Bolometric light curve of 4H89 with additional energy input from a central pulsar. The thick solid line shows the case all γ-rays from the decay of the 0.075 $M_\odot$ ^{56}Co are thermalized.

6. CONCLUSIONS

We have shown that the observed light curve of SN 1993J, which has two maxima, can be well reproduced by the explosion of a red supergiant whose H/He envelope mass has been decreased below ~ 0.9 $M_\odot$. The first maximum of the light curve is due to shock heating of the thin envelope, while the second maximum is due to the radioactive decay of ^{56}Co. Such a small mass envelope is also suggested from the model for the X-ray emission from SN 1993J (Suzuki et al. 1993). The mass of ^{56}Ni synthesized in SN 1993J is ~ 0.08 $M_\odot$ with a factor of ~ 2 possible uncertainty. The light curve features, in particular, the date of the minimum and the decline rate of the tail suggest that substantial ^{56}Ni was mixed into helium layers as has been predicted for SNe Ib/Ic (Shigeyama et al. 1990; Hachisu et al. 1991, 1993). We also calculate the light curves of line γ-rays from ^{56}Ni–^{56}Co decays and the Compton-degraded hard X-rays; we then discuss the possibility of those lines being observed with the *Compton Gamma-Ray Observatory.*

The progenitor's main-sequence mass is estimated to be $\sim$12–15 $M_\odot$ and cannot exceed ~ 20 $M_\odot$ to have the second maximum around day 20. This suggests that the progenitor was a member of a binary system and lost its envelope to the companion star in a more-or-less conservative mass transfer phase. Constraints on the mass, radius and the abundance of the thin envelope from the light curve modeling would be useful to chart the evolution of the binary progenitor.

The relatively small mass progenitor implies that the collapsed object is likely a neutron star rather than a black hole. If the pulsar luminosity in the 1 keV to 10 MeV range exceeds 3×10^{38} ergs s^{-1}, the emitted X-rays could be observed with ASCA within its lifetime. Observations of the pulsar with future missions such as ASTRO-E will be more promising.

We would like to thank Brian Schmidt, Alex Filippenko, Stan Woosley, and Taichi Kato for sending us useful e-mail information on SN 1993J, and Izumi Hachisu and Kohichi Iwamoto for discussion. This work has been supported in part by the Grant-in-Aid for Scientific Research (04640265, 0524-102, 05242207, 2539, 2780) of the Ministry of Education, Science, and Culture in Japan.

REFERENCES

Arnett, W. D. 1982, ApJ, 253, 785
Colella, P., & Woodward, P. R. 1984, J. Comput. Phys., 54, 174
Doggett, J. B., & Branch, D. 1985, AJ, 90, 2303
Filippenko, A. V. 1988, AJ, 96, 1941
———. 1993a, IAU Circ., No. 5731
———. 1993b, IAU Circ., No. 5737
Filippenko, A. V., & Matheson, T. 1993, IAU Circ., No. 5787
Fransson, C., & Kozma, C. 1993, ApJ, 408, L25
Garcia, F. 1993, IAU Circ., No. 5731
Garnavich, P., & Ann, H. B. 1993, IAU Circ., No. 5731; corriegendum: IAU Circ., No. 5733
Hachisu, I., Iwamoto, K., Matsuda, T., Nomoto, K., & Shigeyama, T. 1994, in preparation
Hachisu, I., Matsuda, T., Nomoto, K., & Shigeyama, T. 1991, ApJ, 368, L27
———. 1993, A&AS, submitted
Hashimoto, M., Iwamoto, K., & Nomoto, K. 1993, ApJ, 414, L105
Humphreys, R. M., Aldering, G. S., Bryja, C. O., & Thurmes, P. M. 1993, IAU Circ., No. 5739
Inoue, H., Hayashida, K., Itoh, M., Kondo, H., Mituda, K., Takeshima, T., Yoshida, K., & Tanaka, Y. 1991, PASJ, 43, 213
Johnson, W. N., et al. 1993, ApJS, 86, 693
Kumagai, S., Nomoto, K., Shigeyama, T., Hashimoto, M., & Itoh, M. 1993, A&A, 273, 153
Kumagai, S., Shigeyama, T., & Nomoto, K. 1991, in SN 1987A and Other Supernovae, ed. I. J. Danziger (Garching: ESO), 203
Kumagai, S., Shigeyama, T., Nomoto, K., Itoh, M., Nishimura, J., & Tsuruta, S. 1989, ApJ, 345, 412
Nomoto, K., & Hashimoto, M. 1988, Phys. Rep., 63, 13
Nomoto, K., Kumagai, S., & Shigeyama, T. 1991, in AIP Conf. Proc. 232, Gamma-Ray Line Astrophysics, ed. P. Durouchoux & N. Prantzos (New York: AIP), 236
Nomoto, K., Suzuki, T., Shigeyama, T., Kumagai, S., Yamaoka, H., & Saio, H. 1993, Nature, 364, 507
Perelmuter, J.-M. 1993, IAU Circ., No. 5736
Podsiadlowski, Ph., Hsu, J. J. L., Joss, P. C., & Ross, R. R. 1993, Nature, 364, 509
Saio, H., Kato, M., & Nomoto, K. 1988a, ApJ, 331, 388
Saio, H., Nomoto, K., & Kato, M. 1988b, Nature, 334, 508
Schmidt, B., et al. 1993, Nature, 364, 600
Shigeyama, T., & Nomoto, K. 1990, ApJ, 360, 22
———. 1991, in Supernovae, ed. S. E. Woosley (Berlin: Springer), 198
Shigeyama, T., Nomoto, K., Tsujimoto, T., & Hashimoto, M. 1990, ApJ, 361, L23
Schönfelder, V., et al. 1993, ApJS, 86, 657
Suzuki, T., Kumagai, S., Shigeyama, T., Nomoto, K., Yamaoka, H., & Saio, H. 1993, ApJ, 419, in press
Tanaka, Y. 1993, IAU Circ., No. 5753
Taniguchi, Y., Murayama, T., Sato, Y., Yadoumaru, Y., Ohyama, Y., Kosugi, J., Yoshida, M., & Kurakami, T. 1993, PASJ, 45, L43
The, L. S., Clayton, D. D., & Burrows, A. 1991, in Wolf-Rayet Stars and Interrelations with Other Massive Stars in Galaxies, ed. K. A. Van der Hucht & B. Hidayat (Dordrecht: Kluwer), 485
Thielemann, F.-K., Nomoto, K., & Hashimoto, M. 1993, in Supernovae (Les Houches, Session LIV), ed. J. Audouze et al. (New York: Elsevier), in press
Tweedy, R. W., Balonek, T. J., Hintz, E., Joner, M., Joner, L., & Wells, L. A. 1993, IAU Circ., No. 5817
van Driel, W., et al. 1993, PASJ, in press
Woosley, S. E. 1991, in Supernovae, ed. S. E. Woosley (Berlin: Springer), 202
———. 1993, private communication
Woosley, S. E., Pinto, A., & Ensman, L. M. 1988, ApJ, 324, 466

Note added in proof.—After submitting this paper, we have received preprints by Woosley et al. (Woosley, S. E., Eastman, R. G., Weaver, T. A., & Pinto, P. A., ApJ, submitted [1994]), Herant & Woosley (Herant, M., & Woosley, S. E., ApJ, submitted [1994]), Wheeler et al. (Wheeler, J. C., et al., ApJ, submitted [1994]), Swartz et al. (Swartz, D. A., Clocchiatti, A., Benjamin, R., Lester, D. F., & Wheeler, J. C., Nature, 365, 232 [1993]), Bartunov et al. (Bartunov, O. S., Blinnikov, S. I., Pavluk, N. N., & Tsvetkov, D. Yu., A&A, submitted [1994]), and Hoflich et al. (Hoflich, P., Langer, N., & Duschinger, M., A&A, 275, L29 [1993]). These papers studied light curves and/or mixing as in our paper, and the comparison of these results are seen in Wheeler & Filippenko (Wheeler, J. C., & Filippenko, A. V., in IAU Colloq. 145, Supernovae and Supernova Remnants, ed. R. McCray and Z. Wang [Cambridge: Cambridge Univ. Press], in press [1994]).